Comparison of thermal and piezoresistive sensing approaches for atomic force microscopy topography measurements

William P. King[a)]
Woodruff School of Mechanical Engineering, Georgia Institute of Technology, Atlanta, Georgia 30332

Thomas W. Kenny and Kenneth E. Goodson
Department of Mechanical Engineering, Stanford University, Stanford, California 94305

(Received 24 February 2004; accepted 29 June 2004)

Atomic force microscope cantilevers with integrated piezoresistive displacement sensors are widely used for nanometer-scale topographic measurement and force sensing. Heated cantilevers used in thermomechanical data storage are a promising alternative for topographic measurement. For both cantilever types, this letter models and predicts cantilever displacement sensitivity and noise-limited displacement resolution. The predictions for the thermal cantilever sensitivity compare well with data. Comparing the thermal cantilever with a similarly sized piezoresistive cantilever, the thermal cantilever provides more than one order of magnitude improved performance in both sensitivity and resolution over the piezoresistive cantilever. © *2004 American Institute of Physics*.
[DOI: 10.1063/1.1787160]

Micromachined cantilevers have become widely employed for atomic force microscope (AFM) measurement of surface topographic information.[1] Displacement of the cantilever is typically detected by the movement of a reflected laser beam on a photodetector. Optical methods can become inconvenient where many cantilevers operate in parallel, and so cantilevers with integrated displacement sensors are used for large parallel arrays. The most common approach for integration is with piezoresistive strain sensors.[2] Another approach for integrating the sensor into the cantilever is in thermomechanical data storage, where a heated cantilever detects data bits by measuring temperature changes that correspond to changes in the cantilever–substrate thermal resistance,[3] shown in Fig. 1. Recent work measured and modeled the mechanism of data reading,[4] which aided the design of improved cantilevers.[5] While their sensing mechanisms are fundamentally different, both cantilever types have a sensitivity and resolution that depends upon the electrical and thermal characteristics of the cantilever. This letter models the operation of thermal and piezoresistive cantilevers of nearly identical size and shape, and for a range of electrical operation predicts the sensitivity and resolution of each.

Local probe measurements that depend upon temperature or the flow of heat for microscopy are well known. While the present thermal detection technique is in essence similar to that of the scanning thermal profilometer,[6] the thermal data storage cantilever has a much higher sensitivity due to the differences in heater configuration, operation, and materials properties. In scanning thermal microscopy, temperature maps can be made of surfaces using a thermocouple or thermistor located at the end of the cantilever.[7] Spatial temperature resolution is possible in the 50 nm range.

Thermal detection of "data bit" topography in thermomechanical data storage has resolution governed by the conductance from the cantilever and the size of the tip, which has a radius of curvature of near 20 nm.[8] Previously published work[3] commenting on cantilever reading sensitivity reported $\Delta R/R$ sensitivity of as high as 10^{-3} per vertical nm. The sensitivity of this thermal cantilever is much higher than commercially available piezoresistive cantilevers and thus holds promise as a metrology technique with usefulness beyond data storage. The question that remains is: "What are the limits of extending this data bit reading approach for topographic sensing, and how does this compare to piezoresistive AFM cantilevers?."

In the thermal detection approach for thermomechanical data storage,[3] a resistor in the cantilever is electrically biased so that the cantilever is heated above ambient temperature. This same heating resistor has a temperature coefficient of electrical resistance such that the cantilever temperature can be precisely calibrated and subsequently monitored. The temperature of the cantilever is determined by the heat input and the thermal conduction to the surroundings. The height-dependent conductance from the cantilever heater, G_{heater}, is given as

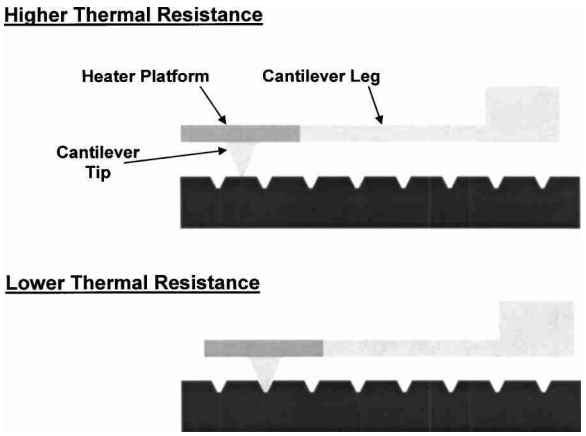

FIG. 1. Thermal reading of surface topography (see Ref. 3). The thermal resistance between the cantilever and the substrate varies as the cantilever tip follows the surface topography, producing a measurable change in the cantilever heating temperature.

[a)]Electronic mail: william.king@me.gatech.edu

$$G_{\text{heater}} = \frac{k_{\text{air}} w_{\text{heater}} l_{\text{heater}}}{z} + 4k_{\text{air}}\left[\frac{w_{\text{heater}} l_{\text{heater}}}{\pi}\right]^{1/2} + 2w_{\text{cant}}\left[\frac{t_{\text{cant}} k_{\text{cant}} k_{\text{air}}}{z}\right]^{1/2}, \quad (1)$$

where k_{air} is the thermal conductivity of the air, w_{heater} is the heater width, l_{heater} is the heater length, z is the cantilever–substrate height, and k_{cant} is the cantilever thermal conductivity of the cantilever. The three terms in Eq. (1) correspond to the thermal conductance from the cantilever heater across the air gap into the substrate, into the air, and along the cantilever legs.[9] Equation (1) assumes that the cantilever is parallel with a flat substrate, that the thermal impedance of the cantilever–substrate air gap is large compared to the thermal impedance in the substrate, and that there is an exponential temperature drop along the length of the cantilever.

The distance between the cantilever heater platform and a surface changes as the cantilever tip scans over a structured surface, resulting in a change in conductance from the cantilever. For a constant heating power, this results in a change in resistance, and also a change in voltage. For operation in series with a resistance equal to the cantilever, the voltage sensitivity is

$$\frac{\partial V}{\partial z} = \frac{-\alpha V_b^3}{8G^2 R}\frac{\partial G}{\partial z}, \quad (2)$$

where α is the temperature coefficient of electrical resistance, V_b is the bridge bias voltage, and R is the cantilever electrical resistance, calculated from solid state models.[10] The parameter α depends upon the doping concentration and type, which at present have not been optimized for improved sensitivity.

For a piezoresistive cantilever operated in series with a resistance equal to that of the cantilever, the voltage sensitivity to small displacements is

$$\frac{\Delta V}{\Delta z} = \beta \pi_L V_b \frac{3Et}{4l^2}, \quad (3)$$

where ΔV is the change in bridge output voltage, Δz is the vertical displacement of the cantilever tip, β is a parameter that varies between zero and unity based upon the piezoresistor doping profile, π_L is the piezoresistive coefficient, E is the cantilever Young's modulus, t is the cantilever thickness, and l is the cantilever length. Typical values are $E \sim 2 \times 10^{11}$ N/m^2,[1] $\pi_L = 72 \times 10^{-11}$ m^2/N,[11] and $\beta = 0.3$.[2]

From Eq. (3), piezoresistive cantilevers can be made more sensitive by increasing the cantilever thickness, decreasing the cantilever length, or operating the cantilever at a higher bias voltage. The piezoresistive coefficient of doped silicon varies inversely with absolute temperature,[12] and thus resistive heating in piezoresistors can reduce their sensitivity. To account for piezoresistor heating, thermal conductance from the piezoresistor, G_{piezo}, is modeled as

$$G_{\text{piezo}} = \frac{k_{\text{air}} w_{\text{piezo}} l_{\text{piezo}}}{z} + 4k_{\text{air}}\left[\frac{l_{\text{piezo}} w_{\text{piezo}}}{\pi}\right]^{1/2} + w_{\text{cant}}\left[\frac{t_{\text{cant}} k_{\text{cant}} k_{\text{air}}}{z}\right]^{1/2} + \frac{\pi k_{\text{cant}} w_{\text{cant}}}{2\ln(4w_{\text{cant}}/t_{\text{cant}})}, \quad (4)$$

where the width and length of the piezoresistors are w_{piezo} and l_{piezo}, respectively. The first three terms of Eq. (4) parallel the first three terms of Eq. (1), while the fourth term corresponds to thermal conduction from the piezoresistor into the substrate.[9]

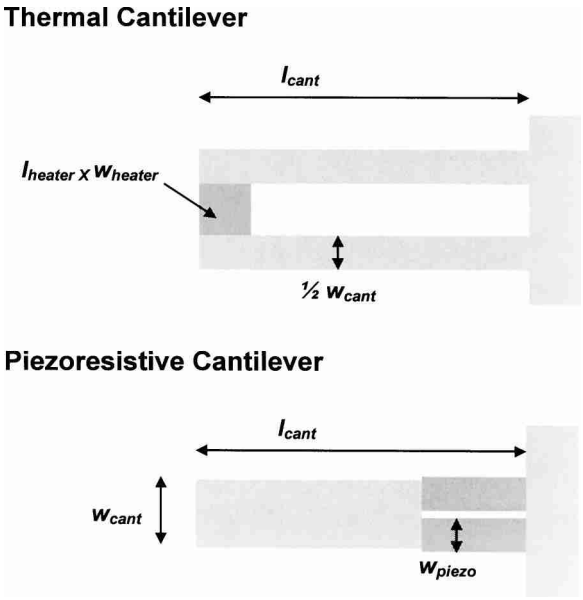

FIG. 2. Illustration of the thermal and piezoresistive cantilever geometry considered in this letter.

The ability to detect small displacements is limited by several factors, including amplifier noise, Johnson noise, thermomechanical noise, and $1/f$ noise. While there are several proposed mechanisms behind $1/f$ noise, it has been shown that a model for this noise offered by Hooge provides an excellent empirical fit to data,[2] and that it competes with Johnson and amplifier noise only for very lightly doped piezoresistors in very thin cantilevers, or at low frequencies, and this analysis neglects it. Amplifier noise is also neglected, although it will be an important practical consideration for both cantilever types. The total thermal and Johnson noise in the cantilevers will have a magnitude[13]

$$V_{\text{noise}} = \sqrt{(\alpha V_b T)^2 \frac{k_B}{G} + 4k_B T R}, \quad (5)$$

where T is the cantilever temperature and k_B is the Boltzmann constant. The first part of Eq. (5) refers to the thermal fluctuation noise, and the second part accounts for Johnson noise. The minimum detectable feature size, z_{min}, is then calculated as the noise divided by the sensitivity.

We choose a previously published thermomechanical data storage cantilever design,[8] and a piezoresistive cantilever of the same overall length, width, thickness, and volumetric doping concentration. Figure 2 shows a schematic of the cantilever footprints, and Table I lists the cantilever dimensions. The design space for both cantilevers is large and the thermal cantilever has not been optimized for topographic mapping, as requirements other than sensitivity are imposed for a data storage application. Optimization of piezoresistive and thermal cantilevers would cause them to diverge in size and shape, and thus comparison of optimal thermal and piezoresistive cantilevers is not strictly fair. In fact, with a higher room-temperature electrical resistance and a piezoresistor length that is one-third of the cantilever length, the piezoresistive cantilever is relatively well optimized for its size[2] and the thermal cantilever is not. How-

TABLE I. Design parameters for the piezoresistive and thermal cantilevers.

Parameter	Piezoresisive cantilever	Thermal cantilever
Length	50 μm	50 μm
Leg width	20 μm	10 μm$\times$2 legs
Thickness	0.2 μm	0.2 μm
Heater size	⋯	5 μm$\times$7 μm
Piezoresistor length	16.3 μm	⋯
Tip height	0.5 μm	0.5 μm
Heater doping	⋯	1×10^{18} cm^{-3}
Leg doping	⋯	1×10^{20} cm^{-3}
Piezoresistor doping	1×10^{18} cm^{-3}	⋯
Doping type	*p*	*n*
Room-temperature resistance	10.9 kΩ	1.6 kΩ

ever, the dimensions of these cantilevers are relatively typical for AFM cantilevers and provide a reasonable starting point for comparison.

Figure 3 shows predictions for the displacement voltage sensitivity for both cantilevers as a function of cantilever heating power. For the thermal cantilever, data available in the literature[4,14] compare well to the present model of thermal cantilever operation. Validation of the piezoresistive sensing model is documented.[2] The shape of the sensitivity–power curve for the thermal cantilever is a combination of the cantilever temperature, temperature-dependent electrical resistance, and conductance. The singularity near 10 mW heating power stems from the temperature dependence of the coefficient of electrical resistivity for the doped silicon cantilever, which changes sign. Overall, the thermal cantilever has one to four orders of magnitude sensitivity improvement over the piezoresistive cantilever.

Figure 4 shows predictions for the resolution limits of both cantilevers. For both cantilevers, the resolution is in the range of 10^{-1}–10^{-4} nm/$\sqrt{\text{Hz}}$, which indicates that sub-nm displacements can be detected with 1 s integration times. The thermal cantilever is predicted to have two to three orders of magnitude resolution improvement over the piezoresistive cantilever. At present, we have not measured the noise-resolution limit of the thermal cantilevers, but the agreement between data and model shown in Fig. 3, and the

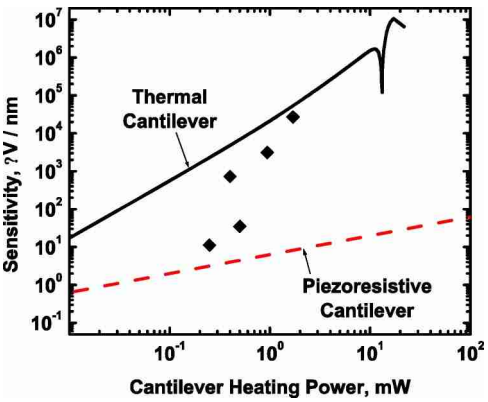

FIG. 3. Predicted voltage displacement sensitivity for the thermal cantilever and for the piezoresistive cantilever. Data are from previously published measurements of cantilevers close in design and operation to the model (Refs. 4 and 14).

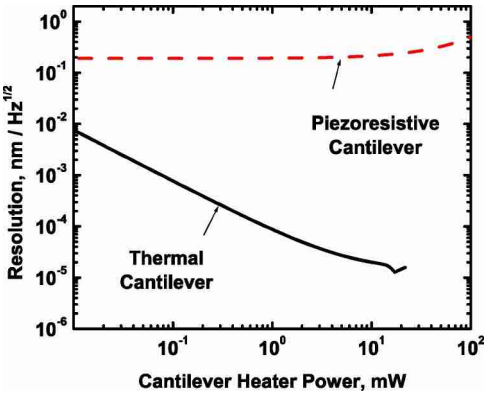

FIG. 4. Predicted minimum detectable feature size for the thermal cantilever and for the piezoresistive cantilever.

simplicity of the noise model provides good confidence for the predictions of Fig. 4.

The improvements offered by thermal over piezoresistive AFM topographic measurement could allow sensitive AFM detection of subangstrom displacements at higher speeds than is currently possible with piezoresistive cantilevers. Much work remains to fully realize the potential of the thermal detection technique. For example, the impact of scanning on surfaces that have topographic features with vertical dimensions comparable to the AFM tip height, or of varying thermal properties could change the cantilever capabilities from those presented here, although not necessarily diminishing them. Applying the thermal detection technique to the measurement of small forces will also require further work, but could provide a very interesting application: Thermal cantilevers become more sensitive as they made thinner, and also have reduced spring constant, which would significantly increase force resolution over piezoresistive cantilevers.

The authors are grateful for the opportunity to collaborate with the Micro/NanoMechanics Group at IBM Zurich Research Laboratory.

[1] G. Binnig, C. F. Quate, and C. Gerber, Phys. Rev. Lett. **56**, 930 (1986).
[2] J. A. Harley and T. W. Kenny, J. Microelectromech. Syst. **9**, 226 (2000).
[3] G. Binnig, M. Despont, U. Drechsler, W. Häberle, M. Lutwyche, P. Vettiger, H. J. Mamin, B. W. Chui, and T. W. Kenny, Appl. Phys. Lett. **76**, 1329 (1999).
[4] W. P. King, T. W. Kenny, K. E. Goodson, G. L. W. Cross, M. Despont, U. Durig, H. Rothuizen, G. Binnig, and P. Vettiger, Appl. Phys. Lett. **78**, 1300 (2001).
[5] W. P. King, T. W. Kenny, K. E. Goodson, G. L. W. Cross, M. Despont, U. Durig, H. Rothuizen, G. Binnig, and P. Vettiger, J. Microelectromech. Syst. **11**, 765 (2002).
[6] C. C. Williams and K. Wickramasinghe, Appl. Phys. Lett. **49**, 1587 (1986).
[7] A. Majumdar, Annu. Rev. Mater. Sci. **29**, 505 (1999).
[8] P. Vettiger, M. Despont, U. Drechsler, U. Dürig, W. Häberle, M. Lutwyche, H. E. Rothuizen, R. Stutz, R. Widmer, and G. Binnig, IBM J. Res. Dev. **44**, 323 (2000).
[9] F. P. Incropera and D. P. DeWitt, *Introduction to Heat Transfer*, 4th ed. (Wiley, New York, 2002).
[10] S. M. Sze, *Physics of Semiconductor Devices* (Wiley, New York, 1981).
[11] Y. Kanda, IEEE Trans. Electron Devices **29**, 64 (1982).
[12] F. J. Morin, T. H. Geballe, and C. Herring, Phys. Rev. **105**, 525 (1957).
[13] F. Reif, *Fundamentals of Statistical and Thermal Physics* (McGraw–Hill, New York, 1965).
[14] G. Cross, M. Despont, U. Drechsler, U. Dürig, P. Vettiger, W. P. King, and K. E. Goodson, Mater. Res. Soc. Symp. Proc. **649**, Q2.3.1 (2001).